Compact Process Model of Temperature Dependent Amorphization Induced by Ion Implantation

Alexander Schmidt, Inkook Jang, Taikyung Kim, Keun-Ho Lee, Young-Kwan Park, Moon-Hyun Yoo, and Chil-Hee Chung

CAE Team, Semiconductor R&D Center
Samsung Electronics Co., Ltd.
San #16, Banwol-Dong, Hwasung-city, Gyeonggi-do, Korea, 445-701
Email: alexander.shmidt@samsung.com

***Abstract*—A compact process model of the thickness of amorphous layer generated by high dose ion implantation was developed. The model takes into account implantation temperature that has strong effect on the damage accumulation and amorphization dynamics. The model is based on the results of Kinetic Monte Carlo simulation of implantation process and provides means for fast and precise calculation of amorphous layer thickness created by most common species used in semiconductor technology, with a wide range of implantation energies, doses and temperatures.**

I. Introduction

Amorphization of silicon substrate induced by high dose ion implantation is widely used in modern silicon technology for the formation of ultra shallow junctions (USJs) as it is beneficial in several ways. Firstly pre-amorphization implantation (PAI) process suppresses ion channeling during following implantation steps, making it easier to create ultra-shallow profiles [1]. Secondly, during solid phase epitaxial regrowth (SPER) [2] which occurs even at low annealing temperatures all defects in amorphized region are removed and transient enhanced diffusion of dopants is strongly retarded. Thirdly, for most of impurities the activation after SPER is higher than the one could be obtained with conventional annealing with the same heat budget [3]. Thus a correct prediction of amorphous layer thickness dependence on the implantation parameters is crucial for a predictive simulation of USJ formation.

Low-temperature implantation seems to be one of the most promising ways to improve silicon amorphization. Implantation with reduced temperatures complicates technology computer-aided design (TCAD) simulations: empirical tables widely used to generate dopant and damage profiles should be completely recalibrated to include temperature effects and existing compact models of amorphization (see, for example [4]) do not take into account temperature effects. The usage of more complicated physical models is also hampered, as a simulation methodology used to obtain amorphous layer thickness should not demand too much computational resources otherwise its practical use for TCAD applications will not be possible. Thus, a development of a compact process model of amorphization that takes into account implantation temperature as well as dose and energy is an important task for improvement of TCAD process simulation quality without jeopardizing its performance.

II. Ion Implantation Induced Amorphization

A. Damage Accumulation and Recombination

At the energy range used in modern semiconductor technology implanted ions propagating through the silicon loose the energy mainly via non-elastic interactions with electrons and elastic interaction with silicon nuclei. The latter leads to the displacement of silicon matrix atoms and generation of vacancies and interstitials. Once the amount of damage exceeds some threshold value (about $1.5 \cdot 10^{22}$ cm^{-3}), silicon is amorphized [2]. Since interstitials and vacancies are highly mobile even at room temperature [5], significant dynamic annealing occurs during implantation process and the thickness of amorphous layer has a strong dependence on the implantation temperature (Fig. 1).

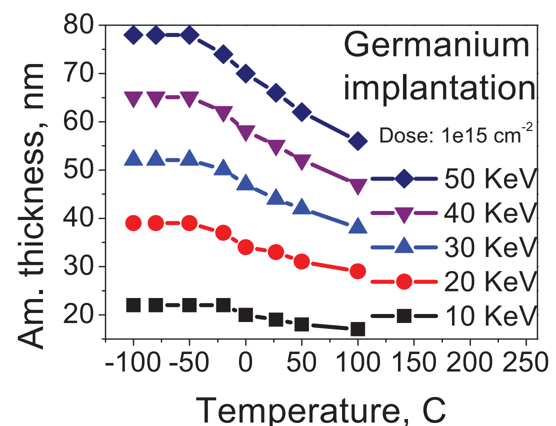

Figure 1. The thickness of an amorphous layer generated by Germanium implantation as a function of implantation temperature and energy. Results of Kinetic Monte Carlo simulation. Dose rate is 10^{12} cm^{-2}s^{-1}.

978-1-4244-7700-5/10/$26.00 ©2010 IEEE

B. Simulation of Amorphization Process

To simulate damage accumulation and amorphization one has to take into account both high energy interactions of incoming ions and matrix atoms and low-energy diffusion processes. Molecular Dynamics simulation, which can do it naturally, has insufficient performance for TCAD usage. Luckily, damage generation and damage recombination have significantly different time scales (picoseconds and microseconds or more, respectively), which allows separate treatment of "instantaneous" damage generation and sequential diffusive recombination. Kinetic Monte Carlo (KMC) method is the most suitable for the task because it allows the simulation of implantation process taking into account dynamic annealing [5], therefore enabling the study of the temperature effect on the amorphous layer formation. Also, KMC uses atomistic approach for diffusion so the deatomization of the data extracted from MC implantation simulations is not needed. The drawback of KMC is large computational time (comparing to continuum simulations).

UT-Marlowe code with the kinetic accumulative damage model [6] and Synopsys Sentaurus Process KMC simulator [7] would be the examples of such approach. Both use binary collisions approximation MC technique for implantation simulation and KMC for diffusion simulation.

C. Calibration of the Kinetic Monte Carlo Model

In present work, simulation was preformed using Synopsys Sentaurus Process tool since its MC implantation and KMC diffusion models have been extensively calibrated for silicon technology [5,7].

For additional confirmation a comparison of the amorphous layer thickness simulation with the in-company and literature experimental data [4] was performed. Good agreement with experimental data is observed for all cases (see an example in Fig. 2).

III. Compact Process Model of Amorphization

A. Model Formulation

Considering fixed ion energy, dose and implantation temperature, amount of damage generated in silicon substrate at a given depth for a given implantation time can be expressed as an integral of a difference between local damage generation and recombination rates (r_g and r_r, respectively):

$$D(x,t,T,E,Dose)= = \int_0^t \left(r_g(x,\tau,E,Dose) - r_r(x,\tau,T,E,Dose)\right)d\tau, \quad (1)$$

x is the depth, t is an implantation time, T is a substrate temperature, E is the implantation energy and $Dose$ is the dose.

As it was shown in [2], damage build-up has non-linear dependence on implantation time (which is equivalent to dose, considering constant dose rate), but if the damage concentration is close to the amorphization threshold T_{am} (about 10^{22} cm^{-3}), linear dependence can be a good approximation, and thus:

$$D(x,t,T,E,Dose)= = G(x,E,Dose)t - R(T)\int_0^t D^2(x,t,T,E,Dose)d\tau, \quad (2)$$

G is constant in time damage generation function and $R(T)$ is a damage recombination coefficient. Equation (1) can be solved, giving:

$$D = \sqrt{\frac{G(x,E,Dose)}{R(T)}} \cdot \tanh\left(t\sqrt{G(x,E,Dose)R(T)}\right). \quad (3)$$

Since we are interested in a high damage limit, hyperbolic tangent function can be ignored, because its value for a large argument is close to one. Thus, assuming long implantation times and large damage generation rate, we can obtain the following relation:

$$D \approx \sqrt{\frac{G(x,E,Dose)}{R(T)}}. \quad (4)$$

To get the amorphous layer thickness from (4) we have to find coordinate x_0, at which the damage is equal to the value of the amorphization threshold. To do so the equation for spatial distribution of the damage should be known. According to the Hobler model [8], Gaussian function can be a good assumption for the damage distribution. Substituting it in (4) we obtain the equation for the amorphous layer thickness in a following form:

$$Dose \cdot a \cdot \exp\left(-\frac{(x_0 - R_p)^2}{4\sigma^2}\right) \Big/ R(T) = T_{am}, \quad (5)$$

where R_p is projected range, σ is standard deviation of a damage profile, a is a normalization factor and x_0 is the amorphous layer thickness. At a fixed energy, the variation of x_0 with a change of the dose is equal to the variation of $x_0 - R_p$, and so this difference may be replaced with x_{am}. Therefore (5) may be rewritten in a following form:

$$-\frac{x_{am}^2(E)}{4\sigma^2(E)} = \ln\left(T_{am}\sqrt{\frac{R(T)}{a}}\right) + \ln(Dose). \quad (6)$$

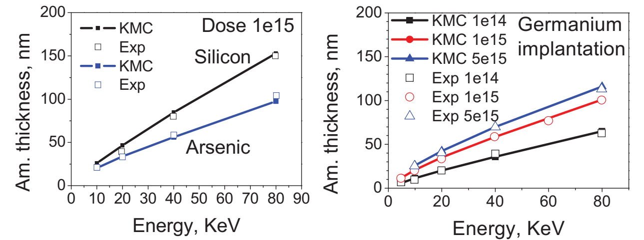

Figure 2. Comparison of KMC simulation results with experimental data: amorphous layer thickness generated by Silicon and Arsenic implantation at dose of 10^{15} cm^{-2} (left) and by Germanium implantation with various doses (right) compared with values extracted from TEM data [4].

Equation (6) is, of course, valid only for implantation doses high enough to make a fully amorphized layer. Finally (6) can be rewritten in a following form:

$$x_{am} = \sqrt{A(T,E) - B(E)\ln\left(\frac{D_0}{Dose}\right)}, \quad (7)$$

where $A(T,E)$, $B(E)$ are the fitting functions, and D_0 is a characteristic dose chosen to be 10^{14} cm^{-2}.

B. Fitting Functions Parameters Values Extraction

Using Sentaurus Process KMC, amorphization processes for energies in a range of 0…50 KeV, doses in a range of 10^{14} cm^{-2}…10^{16} cm^{-2} and temperatures in a range of -100 C…100 C were simulated and the amorphous layer thicknesses were extracted (see example for Germanium implantation in Fig. 3).

For each implantation dose the functions $A(T,E)$, $B(E)$ were extracted (see example in Fig. 4). In the range of interest (implantation temperatures below 100 C), the temperature dependence of $A(T,E)$ is similar to the dependence of total amount of I-V pairs created by implantation, i.e. a Boltzmann function, observed in experiments [9] and simulations [10]:

$$A(E,T) = A_2 + (A_1 - A_2) \Bigg/ \left(1 + \exp\left(\frac{T_0 - T}{Slope}\right)\right), \quad (8)$$

here *Slope* and T_0 variables can be fixed for all energies, leaving A_1 and A_2 to be functions of energy only, since they indirectly represent the dependence of the ion penetration depth on the incidence energy, which is almost insensitive to the temperature. Fig. 5 shows values for A_1 and A_2 as well as their power law fitting. Function $B(E)$ can be also fitted with the power law function (Fig. 3, right panel).

Thus the empirical function for amorphous layer thickness has eight parameters in total (and one constant D_0). The values of these parameters were extracted from KMC simulations using the methodology described above. Parameters for some species, which are often implanted at high doses in modern semiconductor technology, are summarized in Table 1.

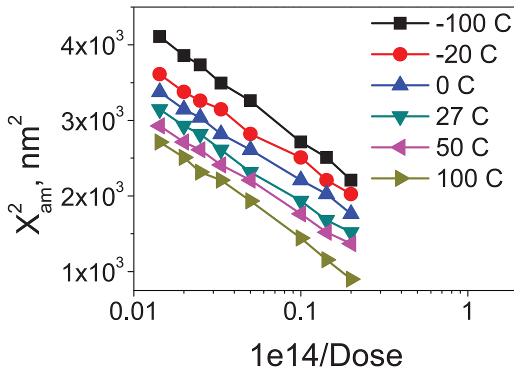

Figure 3. KMC simulation of amorphization thickness created by 30 KeV Germanium implantations at various doses and temperatures. Dose rate is 10^{12} $cm^{-2}sec^{-1}$.

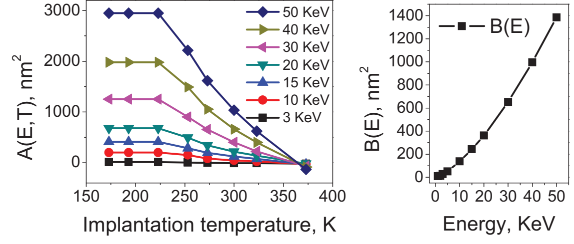

Figure 4. Empirical functions A(T,E) (left) and B(E) (right), extracted from KMC simulations of amorphization induced by Germanium implantation.

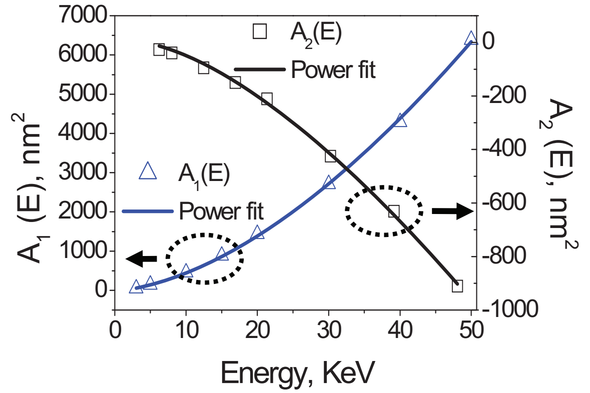

Figure 5. Energy dependence of Boltzmann function parameters A_1 and A_2 for Germanium implantation. Dependencies are fitted with power law functions ($A_1 = 9.72 \cdot E^{1.66}$ nm^2, $A_2 = -2.47 \cdot E^{1.50}$ nm^2, E is implantation energy in KeV).

TABLE I. MODEL PARAMTERS

Specie	Parameter Name, Unit				
	$A_1(E)$, nm^2 (Note a)	$A_2(E)$, nm^2 (Note a)	T_0, K	Tx, K	B(E), nm^2 (Note a)
Ge	$9.72 \cdot E^{1.66}$	$-2.47 \cdot E^{1.50}$	231.7	67.5	$4.62 \cdot E^{1.46}$
As	$8.64 \cdot E^{1.62}$	$-2.46 \cdot E^{1.63}$	266.2	61.6	$3.75 \cdot E^{1.49}$
BF2	$3.42 \cdot E^{1.77}$	$-4.13 \cdot E^{1.65}$	296.4	25.5	$3.47 \cdot E^{1.60}$

a. Energy values are in KeV.

IV. MODEL TESTS AND IMPLEMENTATION

A. Comparison with Experimental and Kinetic Monte Carlo Simulation Results

At first, the results of empirical model were tested against the results of KMC simulation. Fig. 6 shows the residuals between KMC simulation results and function for Arsenic implantation with dose of 10^{15} cm^{-2} at various temperatures and with various energies. In a whole temperature range an error in smaller than 1.5 nm and it is smaller than 1 nm for most of energies. For Arsenic, BF_2 and Germanium root mean square errors of the function results comparing to the values of amorphous layer thickness extracted from KMC simulations are shown in Fig. 7 (results are averaged over temperatures and doses).

The comparison with the experimental data shows almost identical results with KMC simulation.

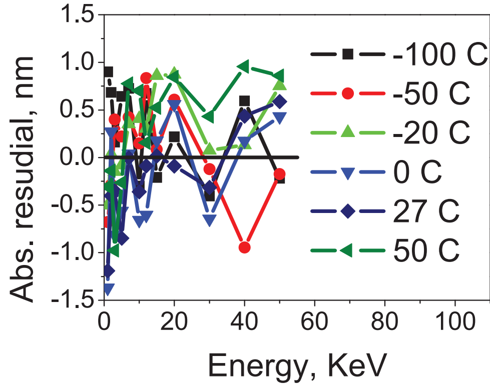

Figure 6. Deviation of the empirical function from KMC simulation results for Arsenic implantation with dose 10^{15} cm^{-2}. For very low implantation energies at which the damage distribution is no longer following Hobler model and so the deviation is higher.

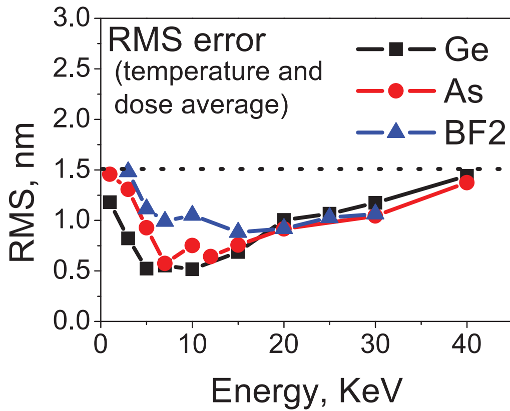

Figure 7. Root mean square error, averaged by doses and temperatures in ranges of $10^{14}\ldots5\cdot10^{15}$ cm^{-2} and -100 ºC…50 ºC. For all species the RMS error is below 1.5 nm.

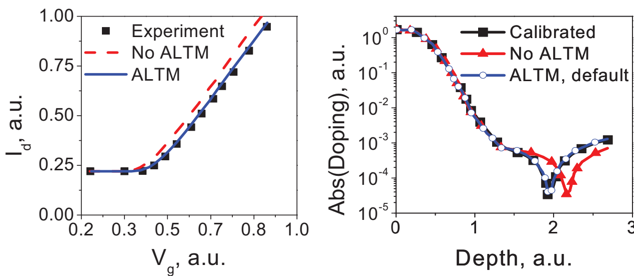

Figure 8. IdVg simulation performed after continuum process simulation with a default calibration parameters with and without implementation of the empirical amorphous layer thickness model (ALTM). Comparison with the experimental data (left). Resulting junction depth is shown on the right panel calibrated process flow without implementation of amorphous layer thickness model and uncalibrated simulation with it provide similar results, but the amount of fitting parameters is reduced from six to just one.

B. *Simulation Preformance Improvement*

Instead of implementation of KMC simulation of implantation steps, the developed compact process model was used in continuum process simulation flow of an advanced DRAM device. This allowed to reduce the amount of process simulation fitting parameters in continuum simulation (due to better prediction of post-implantation defect distribution, see Fig. 8) and significantly reduced simulation time comparing to KMC simulation (implantation and diffusion steps took minutes instead of hours like in regular continuum simulation).

V. Conclusions

For the first time a compact process model of temperature-dependent amorphization induced by high dose ion implantation was developed. Model parameters for the species often used in modern silicon technology were extracted from KMC simulations over a large range of implantation conditions. The precision of amorphous layer thickness obtained from the model is better than 1.5 nm. Implementation of the model to continuum process simulation of advanced DRAM and Logic device manufacturing allows to reduce the number of calibration parameters. Comparing to comprehensive physics based KMC simulations the model has significant performance advantage without a significant precision penalty.

References

[1] E.C. Jones, E. Ishida, "Shallow junction doping technologies for ULSI," Mater. Sci. Eng. R, vol. 24, pp. 1-80, 1998.

[2] L. Pelaz, L. A. Marques, and J. Barbolla, "Ion-beam-induced amorphization and recrystallization in silicon," J. Appl. Phys., vol. 96, no. 11, pp. 5947–5976, 2004.

[3] M. Aboy, L. Pelaz, L. A. Marques, P. Lopez, J. Barbolla, and R. Duffy, "Atomistic analysis of the evolution of boron activation during annealing in crystalline and preamorphized silicon," J. Appl. Phys., vol. 97, no. 10, pp. 103520–103527, 2005.

[4] K. Suzuki, K. Kawamura, Y. Kikuchi, and Y. Kataoka, "Compact model for amorphous layer thickness formed by ion implantation over wide ion implantation conditions," IEEE Trans. Electron Devices, vol. 53, no. 5, pp. 1186-1192, 2006.

[5] N. Zographos, I. Martin-Bragado, "A comprehensive atomistic kinetic Monte Carlo model for amorphization/recrystallization and its effects on dopants," Mater. Res. Soc. Symp. Proc., vol. 1070, 1070-E03-01, 2008.

[6] S. Tian, M. F. Morris, S. J. Morris, B. Obradovic, G. Wang, A. F. Tasch, and C. M. Snell "A detailed physical model for ion implant induced damage in silicon," IEEE Trans. Electron Devices, vol. 45, no. 6, pp. 1226-1238, 1998.

[7] Advanced Calibration User Guide C-2009.06, Mountain View, California: Synopsys, Inc., 2008.

[8] G. Hobler, S. Selberherr, "Two-dimensional modeling of ion implantation induced point defects," IEEE Trans. Computer-Aided Des., vol. 7, no. 2, pp. 174-180, 1988.

[9] P. J. Schultz, C. Jagadish, M. C. Ridgway, R. G. Elliman, and J. S. Williams "Crystalline-to-amorphous transition for Si-ion irradiation of Si(100)", Phys. Rev. B, vol. 44, pp. 9118-9121, 1991.

[10] L. Pelaz, L. A. Marques, M. Aboy, J. Barbolla, and G. H. Gilmer, "Atomistic modeling of amorphization and recrystallization in silicon" Appl. Phys. Lett., vol. 82, no. 13, pp. 2038-2040, 2003.